Bioorganic Chemistry 93 (2019) 103316

Contents lists available at ScienceDirect

Bioorganic Chemistry

journal homepage: www.elsevier.com/locate/bioorg

# Synthesis and anti-tyrosinase mechanism of the substituted vanillyl cinnamate analogues

Zefeng Zhao[a,1], Guangxin Liu[b,1], Yufeng Meng[a], Jiale Tian[a], Xufei Chen[a], Meilun Shen[b], Yuexuan Li[a], Bingyao Li[a], Cong Gao[a], Shaoping Wu[a], Cuiqin Li[b,*], Xirui He[c], Ru Jiang[d], Mingcheng Qian[e,f,*], Xiaohui Zheng[a,*]

[a] School of Pharmacy, Biomedicine Key Laboratory of Shaanxi Province, Northwest University, Xi'an, China
[b] Key Laboratory of the Ministry of Education for Medicinal Resources and Natural Pharmaceutical Chemistry, National Engineering Laboratory for Resource Development of Endangered Crude Drugs in Northwest of China, College of Life Sciences, Shaanxi Normal University, Xi'an, Shaanxi, China
[c] Department of Bioengineering, Zhuhai Campus of Zunyi Medical University, Zhuhai, 519041, China
[d] School of Pharmacy, The Fourth Military Medical University, Xi'an, Shaanxi, China
[e] Department of Medicinal Chemistry, School of Pharmaceutical Engineering and Life Science, Changzhou University, Changzhou 213164, Jiangsu, China
[f] Laboratory for Medicinal Chemistry, Ghent University, Ottergemsesteenweg 460, B-9000 Ghent, Belgium

ARTICLE INFO

*Keywords:*
Inhibitor
Cinnamic acid
Tyrosinase
Docking

ABSTRACT

This study aimed to synthesize and screen tyrosinase inhibitors for delay fruit browning. A series of vanillyl cinnamate analogues were designed and synthesized by simple processes, and the inhibitory effects of all the synthesized derivatives on mushroom tyrosinase were evaluated. In the enzymatic activity test, compounds **21, 22,** and **26** had significant ($P < 0.05$) effect on mushroom tyrosinase at a preliminary screening dose (1 mg/mL *in vitro*). $IC_{50}$ analysis showed that the $IC_{50}$ values of compounds **21, 22** and **26** were 268.5 μM, 213.2 μM and 413.5 μM, respectively. In the cytotoxicity evaluation, Cell Counting Kit-8 (CCK-8) assay showed that compounds **21, 22** and **26** had no significant effect on the proliferation of hepatocyte L02 and B16 melanoma cells at the dosage of 25–200 μM. Inhibition of tyrosinase activity and melanin content in B16 melanoma cells investigations indicated that compounds **21**, **22** and **26** inhibited both cellular tyrosinase activity and melanin content dose-dependently and more strongly than the reference standard arbutin. The UV–visible spectra showed compound **22** inhibits the formation of dopamine quinone, further the molecular docking analysis of compound **22** with tyrosinase (PDB: 2Y9X) indicated that compound **22** interacted with the amino acid residues of tyrosinase. The results of anti-browning test showed that compounds **21, 22** and **26** had significant tyrosinase inhibition and anti-browning effects on fresh-cut apple slices at 4 °C in 48 h. Compound **22** could be used as novel tyrosinase inhibitor to delay fruit browning.

## 1. Introduction

Tyrosinase is a copper-containing metalloenzyme which was widely distributed in plants, animals and microorganisms nature. Tyrosinase derives its name from its substrate L-tyrosine, which catalyzes the conversion of L-tyrosine to 3,4-dihydroxyphenylalanine (L-Dopa), it is further oxidized to dopamine and eventually to melanin [1]. The first promotes the rate-limiting step of the overall melanin biosynthesis consisting in the hydroxylation of tyrosine to DOPA, followed by the oxidation of the latter to DOPA quinine [2]. Tyrosinase could cause browning of fruits, leading to loss of glossy appearance and relish of the fruits [3]. Cytotoxicity, stability and selectivity are the main reasons behind the failure of large of number tyrosinase enzyme inhibitors [4]. Researchers are making the unremitting effort to explore effective tyrosinase inhibitors with side effect as weak as possible.

Natural products are the important source of the precursor of tyrosinase inhibitors. Cinnamic acid (Fig. 1) is a typical constituent from *Cinnamomum cassia* Blume which has been widely used in food industry

*Abbreviations:* CCK-8, Cell Counting Kit-8; DMAP, 4-(dimethylamino)-pyridin; EDCI, 1-(3-Dimethylaminopropyl)- 3-ethylcarbodiimide hydrochloride; 4-HBA, 4-hydroxybenzoic acid; $IC_{50}$, 50% inhibiting concentration; $K_i$, inhibition constant; L-Dopa, 3,4-dihydroxyphenylalanine; TMCA, 3,4,5-trimethoxycinnamic acid; SAR, structure-activity relationship; Vc, vitamin C

* Corresponding authors.
*E-mail addresses:* licuiqin16@snnu.edu.cn (C. Li), qianmingcheng@cczu.edu.cn (M. Qian), zhengxh@nwu.edu.cn (X. Zheng).
[1] The first two authors contributed equally to this article and share co-first authorship.

https://doi.org/10.1016/j.bioorg.2019.103316
Received 16 May 2019; Received in revised form 29 August 2019; Accepted 25 September 2019
Available online 26 September 2019
0045-2068/ 

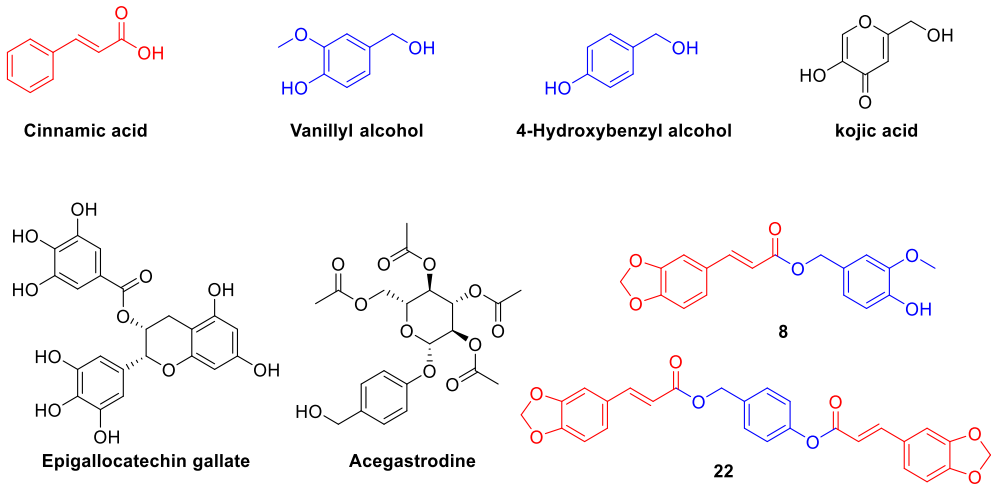


**Fig. 1.** Lead compounds and the designed vanillyl cinnamate analogues.

as additive [5]. The anti-melanin ability of cinnamic acid has been reported and revealed that this compound influenced on the expression level of enzymes related to the enzymes of melanin [6], additionally, the cinnamic acid derivatives have been disclosed to exhibit anti-tyrosinase effect [7–9]. *Gastrodia elata* Blume is a traditional medicinal herb widely utilized in orient area [10], and the anti-melanogenesis ability of *Gastrodia elata* has been explored [11,12]. Vanillyl alcohol is a main constituent from *Gastrodia elata*, and is the intermediate to obtain the extensively used food additive vanillin [10]. Vanillyl alcohol has been report to exert multiple kinds of bioactivities including anti-asthmatic and anticonvulsant, while the tyrosinase inhibiting activity of vanillyl alcohol has not been disclosed. 4-Hydroxybenzyl alcohol, a representative constituent from *Gastrodia elata*, is the intermediate to synthesize gastrodin and 4-hydroxybenzoic acid (4-HBA) [13]. 4-Hydroxybenzyl alcohol is structurally similar to the generally reference drugs kojic acid (5-hydroxy-2-(hydroxymethyl)-4*H*-pyran-4-one) and hydroquinone, and the tyrosinase inhibiting activity of 4-hydroxybenzyl alcohol has been presented [14]. Acegastrodine is a marked sedative drug in China approved by CFDA (H20013040), and is partly similar to the known tyrosinase inhibitory agent arbutin. Ester compounds like epigallocatechin gallate plays important roles in the development of industrial food additive, meanwhile, the antioxidant [15], antibacterial [16] and anti-tyrosinase [17] properties have been widely reported, which proves the rationality of the existing of ester moiety, herein, we design and synthesis a cluster of ester compounds containing the group of precursors to investigate the potential anti-browning agents.

Fresh-cut apples provide customers with freshness, convenience and nutrition [18,19], it is susceptible to be damaged due to enzymatic browning in the process of being cut or peeled. The enzymatic browning is caused by catalytic oxidation under polyphenol oxidase and peroxidase [20]. It is estimated that enzymatic browning causes more than 50% fruit loss [21].

In this study, a series of vanillyl cinnamate analogues (**1–26**) was synthesized and introduced three kinds of the substituted group on the benzene ring of cinnamic acid ($S_1$-$S_3$). Among them, 3,4,5-trimethoxycinnamic acid (TMCA) is an important active constituent from *Polygalae Radix* [22,23]. 3-Methyl-butenyl and acetyl glucose group (Scheme 1) were introduced to form the etherification products of 4-hydroxybenzyl alcohol and vanillyl alcohol. The activity of esterification products of phenolic hydroxyl group on 4-hydroxybenzyl alcohol and vanillyl alcohol using the substituted cinnamic acids has also been discussed (**19–26**).

To furnish the better inhibitors with intriguing structural features, we investigated the pharmacological properties of the synthesized compounds. Most of the synthesized derivatives exhibited moderate inhibitory activity in the test dosage. The strategy of combining kinetics, UV–visible spectra and molecular docking facilitate the elaboration of the inhibitory mechanism. Furthermore, the most promising compound is studied as an effective preservative to delay the browning of fresh-cut apples.

## 2. Results and discussions

### 2.1. Mushroom tyrosinase inhibition

The whole synthesized compounds were evaluated to validate their role as tyrosinase enzyme inhibitors. Kojic acid was used as a standard and the results obtained as inhibition (%) value are summarized in Table 1. Interestingly, except for compounds **20** and **24**, most of the synthesized compounds exhibited inhibition potential against mushroom tyrosinase at the dose of 1 mg/mL. Furthermore, active compounds **4, 5, 8, 21, 22, 23** and **26** which exhibited favorable inhibitory effect with the values more than 40% in the initial screen were selected from the preliminary screen to measure the $IC_{50}$ values (Table 2). All the tested compounds showed much better potential compared to standard kojic acid. The compound **22** was found to be a dominant inhibitor compared to other derivatives in the series with $IC_{50}$ value of 213.2 μM.

As for the structure-activity relationship, firstly, we consider that the non-methoxyl substituted on the C-3 on the benzene ring of vanillyl moiety is good for activity (Fig. 2). It is obviously that the potential inhibition of 4-hydroxybenzyl alcohol analogues is better for vanillyl alcohol analogues according to the test results, which is relative to the structural similarity between 4-hydroxybenzyl alcohol and hydroquinone. Secondly, the rank of activity for the different substituted groups on cinnamic acid: 3,4-dioxymethyl > 3,4-dimethoxyl > non-substituted > 3,4,5-trimethoxyl. Typical potential compounds **21** and **22** contain 3,4-dimethoxyl or 3,4-dioxymethyl group in structure, while 3,4,5-trimethoxyl cinnamic acid analogues performed weak inhibition in test, revealing that substituted groups of C-3 and C-4 on the benzene ring of cinnamic acid are indispensable for the anti-tyrosinase activity, which is corresponding to the know active anti-tyrosinase agents ferulic acid and caffeic acid. Thirdly, the substituted cinnamyl group on phenolic hydroxyl group of vanillyl moiety is helpful to promote activity, while 3-methyl-butenyl and acetyl-glucopyranosyl etherification may have diminished its activity. We can deduce this argument by comparing the activity of compounds **4** and **22**, **4** and **18**, respectively.

### 2.2. Cytotoxicity of compounds *21, 22* and *26*

As we should see in Fig. 3, the cytotoxicity of compounds **21**, **22** and

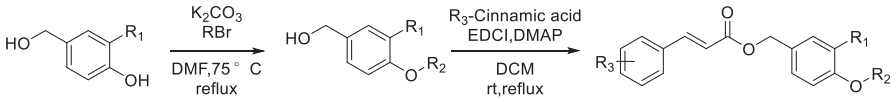


| Com. | $R_1$ | $R_2$ | $R_3$ | Com. | $R_1$ | $R_2$ | $R_3$ |
|---|---|---|---|---|---|---|---|
| **1** | H | H | H | **10** | H | a | $S_1$ |
| **2** | H | H | $S_1$ | **11** | H | a | $S_2$ |
| **3** | H | H | $S_2$ | **12** | H | a | $S_3$ |
| **4** | H | H | $S_3$ | **13** | OMe | a | H |
| **5** | OMe | H | H | **14** | OMe | a | $S_1$ |
| **6** | OMe | H | $S_1$ | **15** | H | b | H |
| **7** | OMe | H | $S_2$ | **16** | H | b | $S_1$ |
| **8** | OMe | H | $S_3$ | **17** | H | b | $S_2$ |
| **9** | H | a | H | **18** | H | b | $S_3$ |

a:

b:

$S_1$: 3,4,5-Trimethoxyl

$S_2$: 3,4-Dimethoxyl

$S_3$: 3,4-Dioxymethyl

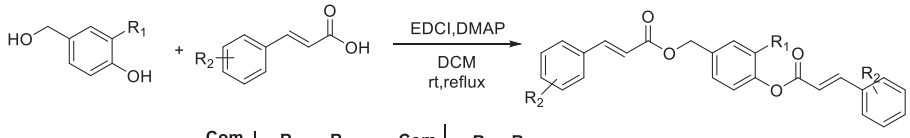


| Com. | $R_1$ | $R_2$ | Com. | $R_1$ | $R_2$ |
|---|---|---|---|---|---|
| **19** | H | H | **23** | OMe | H |
| **20** | H | $S_1$ | **24** | OMe | $S_1$ |
| **21** | H | $S_2$ | **25** | OMe | $S_2$ |
| **22** | H | $S_3$ | **26** | OMe | $S_3$ |

**Scheme 1.** Synthesis of the vanillyl cinnamate analogues derivatives.

**Table 1**
Measured results of target compounds (1 mg/mL) on enzymatic-based tyrosinase activity inhibition percentage.

| Com. | Inhibition (%) ± SD | Com. | Inhibition (%) ± SD | Com. | Inhibition (%) ± SD | Com. | Inhibition (%) ± SD |
|---|---|---|---|---|---|---|---|
| **Kojic acid** | 86.7 ± 2.4* | **7** | 31.3 ± 2.0 | **14** | 9.5 ± 1.0 | **21** | 84.7 ± 1.7* |
| **1** | 15.4 ± 0.4 | **8** | 48.0 ± 1.5* | **15** | 17.8 ± 1.4 | **22** | 91.6 ± 2.2* |
| **2** | 36.4 ± 1.8 | **9** | 12.0 ± 2.1 | **16** | 19.1 ± 0.8 | **23** | 62.8 ± 2.0* |
| **3** | 33.2 ± 1.1 | **10** | 11.5 ± 1.5 | **17** | 11.1 ± 1.0 | **24** | −4.8 ± 0.5 |
| **4** | 66.8 ± 1.5* | **11** | 15.8 ± 1.2 | **18** | 12.4 ± 2.8 | **25** | 42.6 ± 1.1 |
| **5** | 51.4 ± 2.3* | **12** | 27.8 ± 0.7 | **19** | 11.7 ± 1.9 | **26** | 75.9 ± 1.2* |
| **6** | 16.7 ± 0.9 | **13** | 14.7 ± 1.3 | **20** | −2.5 ± 0.3 | | |

**Notes:** Values represent the mean ± standard deviation (SD) of mushroom tyrosinase inhibition experiments (n = 3). Values followed by * are statistical different at $P < 0.05$, according to Tukey test.

**26** was evaluated on the proliferation of normal liver cells L02 and (Fig. 3A) and B16 melanoma cells (Fig. 3B), the cells were treated with 0, 25, 50, 100, 200 and 400 μM of the test compounds for 24 h, respectively. Compounds **21**, **22** and **26** exerted weak cytotoxicity (< 10%) against normal liver cell L02 and B16 melanoma cells at the dosage of 200 μM, suggesting the safety of synthetic derivatives.

**Table 2**
Measured results of $IC_{50}$ values for active compounds on enzymatic-based tyrosinase activity inhibition.

| Com. | $IC_{50}$ (μM) | Com. | $IC_{50}$ (μM) |
|---|---|---|---|
| **Kojic acid** | 1145 | **8** | > 1000 |
| **4-Hydroxybenzyl alcohol** | 365.8 (311.9–443.2) | **21** | 268.5 (198.7–323.4) |
| **Cinnamic acid** | > 1000 | **22** | 213.2 (165.0–231.9) |
| **4** | > 1000 | **23** | 669.7 (483.3–721.7) |
| **5** | > 1000 | **26** | 413.5 (355.2–441.1) |

### *2.3. Cellular tyrosinase inhibitory activity of compounds **21, 22** and **26***

Based on the results exhibited in Fig. 4, compounds **21, 22** and **26** were proved to effectively suppressed the activity of cellular tyrosinase in B16 melanoma cells in a dose-dependent manner. Among the tested active compounds, compound **21** (inhibition: 48.4%) and **22** (inhibition: 45.6%, Fig. 5) showed the remarkable cellular tyrosinase inhibitory activity compared to the moderately active compound **26** (inhibition: 26.9%) at the dose of 200 μM. Both the compounds **21** and **22** displayed better inhibitory effect than the reference arbutin (28.2%, 1 mM). The sequence of the activity for compounds was consistent with the result in enzyme inhibition determination and the deduction from

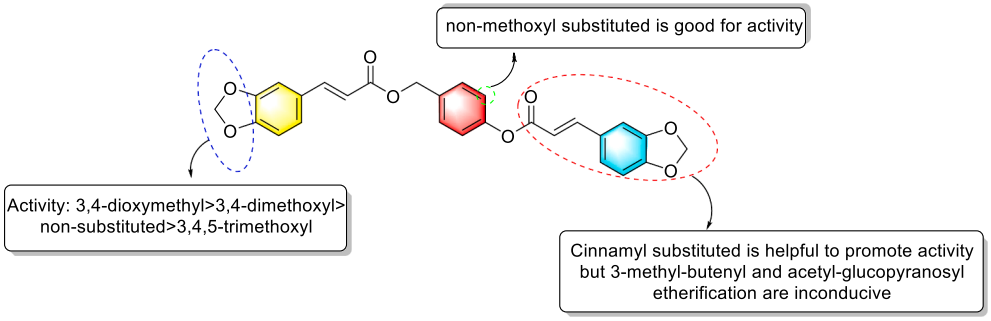


**Fig. 2.** Preliminary structure-activityrelationship (SAR) of the synthesized derivatives.

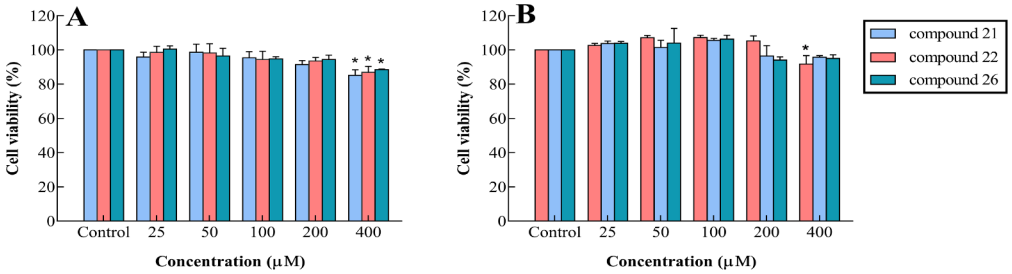


**Fig. 3.** Cell viability (%) of normal liver cell L02 (A) and B16 melanoma cells (B) after 24 h of treatment with compounds **21**, **22** and **26**. Each value is presented as the mean ± standard deviation (SD). Significant difference with control group: $^{*}p < 0.05$.

the SAR research. Considering that the active vanillyl cinnamate analogues did not show cytotoxicity at concentrations below 400 μM, as shown in Fig. 3, the inhibition of tyrosinase activity was attributed to direct tyrosinase inhibition by the analogues, rather than cytotoxicity. The esterification on the C-4 position vanillyl moiety promoted the hydrophobic character and the liposolubility, thus favoring its permeation through the lipoid layer of the cell membrane.

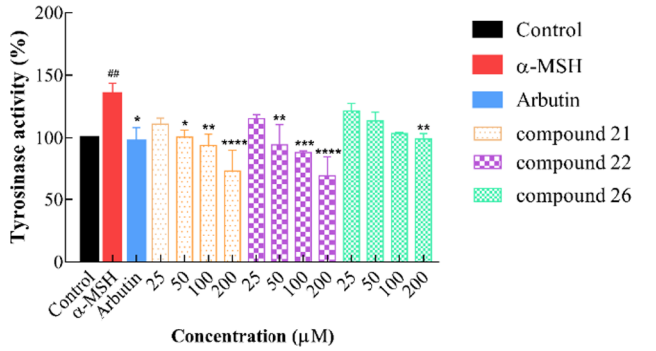


**Fig. 4.** Cellular tyrosinase inhibitory activity of compounds **21, 22** and **26** in B16 melanoma cells. Notes: *: $p < 0.05$, **: $p < 0.01$, ***: $p < 0.001$, ****: $p < 0.0001$ (compared with model group), ##: $p < 0.01$ (compared with control group).

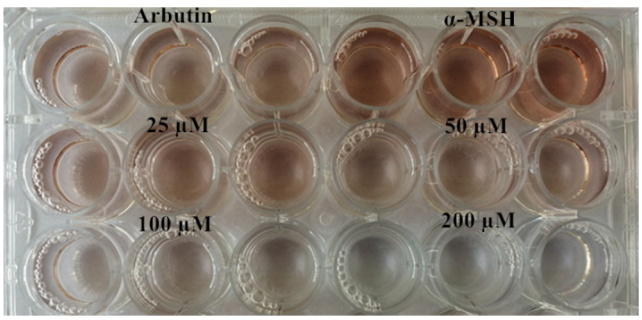


**Fig. 5.** Cellular tyrosinase inhibitory activity of the most promising compound **22** at different concentrations.

### 2.4. Melanin production inhibitory effect of compounds *21, 22 and 26*

The similar result was observed in the melanin production inhibitory effect test between the inhibition of tyrosinase activity (Fig. 6). Compounds **21, 22** and **26** suppressed the melanin production with the inhibition ratio values of 42.0%, 44.2% and 30.41%, respectively. These results provided evidences that inhibition of melanin production was due to inhibition of tyrosinase activity by the active vanillyl cinnamate analogues.

### 2.5. Kinetic mechanism

Kinetic studies were carried out to investigate the inhibitory mechanism of active compounds on tyrosinase inhibition. According to $IC_{50}$ values, we pick up our most promising compounds **21**, **22** and **26** to evaluate their inhibition constant and inhibition type. The inhibitory effects of different concentrations of compounds **21** (**A**), **22** (**B**) and **26** (**C**) on the oxidation of L-Dopa by mushroom tyrosinase were studied Fig. 7. The line Fig. 7(a) showed that under different concentrations of compounds, the residual enzyme activity shows a series of straight lines along the curve of enzyme concentration, and these straight lines all passed through the origin. The slope of the curve shows downtrend with the increase of the inhibitor concentration indicating that the inhibitory mechanism by compounds on diphenolase was reversible [24].

A kinetic study was conducted to explore the inhibition type of compounds **21**, **22** and **26** on tyrosinase by Line weaver-Burk plot analysis as shown in the line Fig. 7(b). A series of straight lines intersected at a point in the second quadrantindicating that compounds **21** and **22** were mixed type inhibitors with a $K_i$ value of 7.7 nM and 18.3 nM, and Kis value of 3.6 nM and 4.4 nM, respectively [25]. The $K_i$ value and $K_{is}$ value was calculated from the plot of the slope in the line Fig. 7(c) and intercept the line Fig. 7(d) versus inhibitor concentrations. And the $K_i$ value of inhibitor larger than their $K_{is}$ value, indicating that the affinity of the inhibitors for the enzyme-substrate complex was greater than that for the free enzyme [26]. And the series of straight

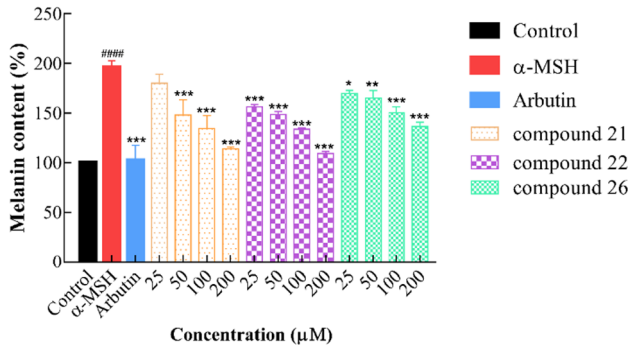


**Fig. 6.** Melanin production inhibitory effect of compounds **21, 22** and **26** in B16 melanoma cells. Notes: *: $p < 0.05$, **: $p < 0.01$, ***: $p < 0.001$, ****: $p < 0.0001$ (compared with model group), ##: $p < 0.01$ (compared with control group).

lines interected at a point on the ordinate indicating that compound **26** was competitive inhibitor with a $K_i$ value of 6.1 nM [27]. For the mix-type inhibitor, it binds not only the enzyme substrate complex, but also to free enzyme, but the competitive inhibitor only binds to the free enzyme.

### 2.6. Effect of compound 22 on UV–visible spectra of tyrosinase

Effect of the most active compound **22** located in the active center of tyrosinaseon UV–visible spectra of tyrosinase dinuclear copper ions, which plays a fundamental role in the catalytic process by interacting with oxygen molecular. The direct interaction of the compound **22** with the copper ion was also assessed (Fig. 8A). The peak height of inhibitor decreased gradually with the increase of copper ion concentration, indicating that the compound **22** could bind to tyrosinase. Moreover, the peaks then returned to their original absorption maxima in the presence of ethylenediaminetetraacetic acid (EDTA). The increase of inhibitor concentration with the reduction of peak at 475 nm (Fig. 8B), indicated the compound **22** can effectively decrease the production of dopamine quinone.

### 2.7. Inhibitory effects of compounds 21, 22 and 26 on the browning of fresh-cut apple slices

In general, $L^*$, $a^*$ and $b^*$ have been adopted as the most critical parameters for prevention the extent of browning in fruits. Lower $L^*$ and higher $a*$ values indicate that the products become darker. Previous studies revealed that the combined effect of Vc (vitamin C) and compounds or plants extracts on maintaining quality of fresh-cut apples and exhibiting better anti-browning effects [28]. Herein, we chose $L^*$ value as marker parameters to assess the anti-browning capability of the tested compounds. The initial $L^*$ values of all the groups were equal statistically and they tended to reduce with storage time extension. Different treatments of water, Vc, 4-hydroxybenzyl alcohol, vanillyl alcohol, cinnamic acid, compounds (**21**, **22** and **26**), and compounds (**21**, **22** and **26**) in combination with Vc were assayed for anti-browning effect on fresh-cut apple slices. Based on the change of $L^*$ values, the apples treated with water almost did not show anti-browning effect. Additionally, 4-hydroxybenzyl alcohol (Fig. 9A and C) and vanillyl alcohol (Fig. 9B) not only did not show the effect of anti-browning, but also appeared to aggravate the phenomenon of browning compared to water. Browning of fresh-cut fruits provoked by slicing and peeling due to the tissue damage, which includes non-enzymatic and enzymatic browning reactions during storage and processing [29]. This phenomenon could be related to other factors other than tyrosinase, but

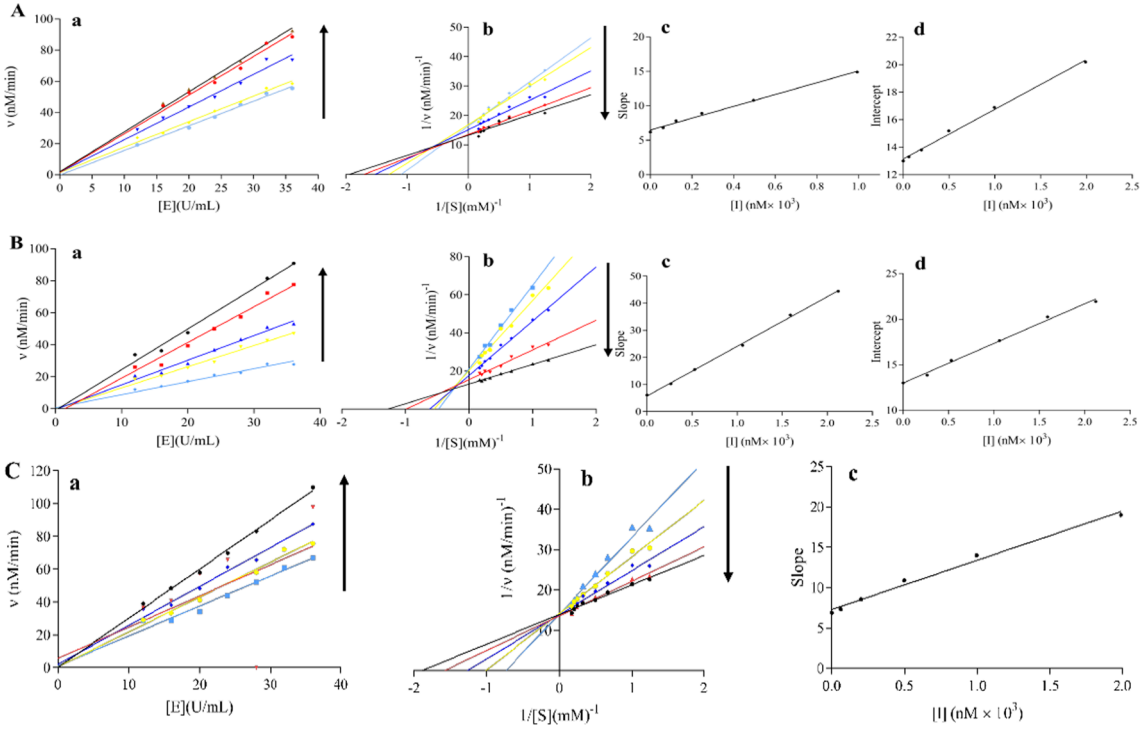


**Fig. 7.** Inhibition of compound **21** (A), compound **22** (B) and compound **26** (C) on diphenolase activities of mushroom tyrosinase. (a) Effects of tyrosinase concentrations on its diphenolase activities at different concentrations of inhibitors. The concentrations of compound **21**, **22** and **26** for curves were 0, 0.12, 0.24, 0.5, and 1.0 μM (follow the sequence of arrows). (b) Lineweaver-Burk plots for mushroom tyrosinase with L-Dopa as substrate in the presence of compound **21, 22** and **26**. The concentrations of compound **21**, **22** and **26** for curves were 0, 0.12, 0.24, 0.5, and 1.0 μM (follow the sequence of arrows). The final enzyme concentration was 24 U/mL. (c) The secondary replot represents the slope versus compound **21, 22** and **26** to determine the inhibition constant $K_i$. (d) The secondary replot represents the interscept versus compound **21, 22** and **26** to determine the inhibition constant $K_{is}$. The abbreviation $\nu$ represent the rate of enzyme reaction. And the abbreviation U is the unit of enzyme activity, which means the amount of enzyme to transform 1 μM substrates in 1 min.

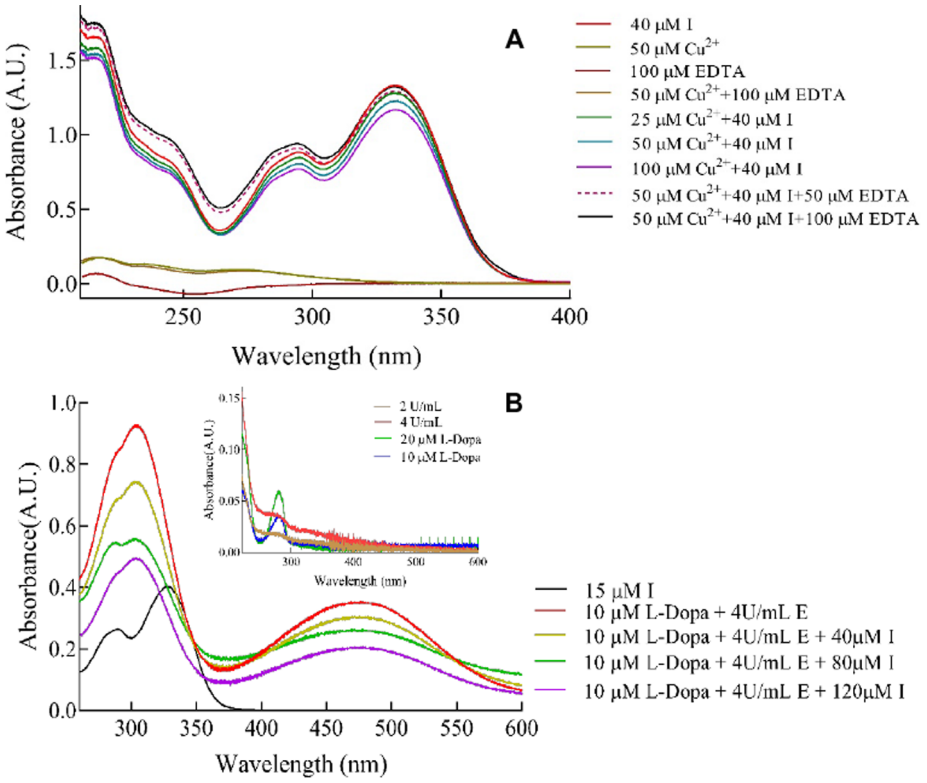


**Fig. 8.** UV–visible spectra for the interaction between compound **22** and tyrosinase. (A) Absorption spectra for compound **22** upon the addition of different concentrations of $CuSO_4$ as well as EDTA. (B) Absorption spectra of tyrosinase in the absence and presence of compound **22**. The abbreviation E represents the tyrosinase. The meaning of U is the unit of enzyme activity.

its mechanisms still need to be studied. Vc is better at preservation than cinnamic acid, while compounds **21**, **22** and **26** alone showed much better anti-browning effect than Vc (Fig. 9A, B, C). Compounds **21**, **22** and **26** in combination with 0.5% $V_C$, respectively, exhibited significant anti-browning effects, better than compounds **21**, **22** and **26** alone, and compound **22** + 0.5%$V_C$ was the most effective.

Although the anti-browning mechanism of active compounds has not been reported, the above results suggested the browning inhibition of compounds may be accomplished through a mechanism similar with inhibition of tyrosinase. The finding preliminarily demonstrate that the active compounds could be potential preservative as anti-browning agents for fresh-cut fruits (Fig. 10).

### 2.8. Molecular docking analyses

The construction of molecular and the analysis of docking between 2Y9X and tropolone, kojic acid, the active compounds **21, 22** and **26** were possessed as delineated in the subsequent section. The

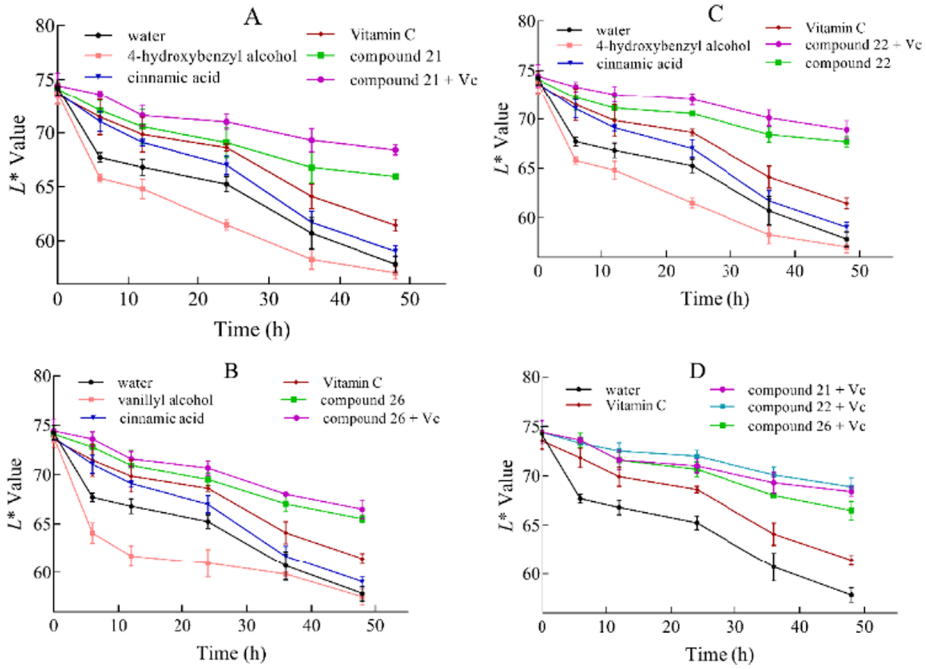


**Fig. 9.** Reflectance measurement of *L** of fresh-cut apple treated with the different tested solutions and stored at refrigerator at 4 °C in 0–48 h. The final concentration of all compounds was 2 mM.

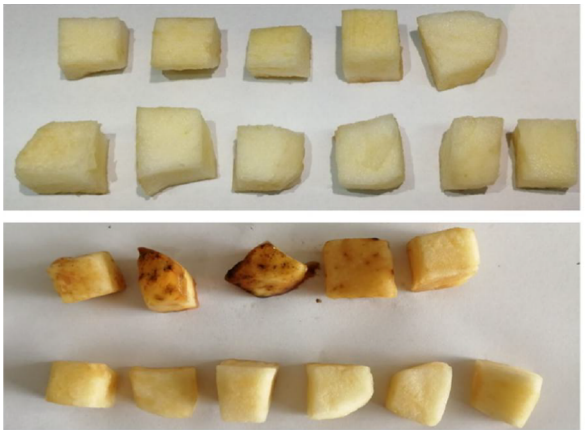


**Fig. 10.** Anti-browning effect of test compounds protecting against fresh-cut apples (correspondence of possess on the test apple pieces from left to right: first line: water, vanillyl alcohol, 4-hydroxybenzyl alcohol, cinnamic acid and Vc; second line: compound **21**, compound **21** + Vc, compound **22**, compound **22** + Vc, compound **26** and compound **26** + Vc).

computationally predicted lowest energy complex is stabilized by the intermolecular hydrogen bonds and stacking interactions. The steric bulk and type of functional groups determine the interactions in the complex. The binding affinity of the enzyme-inhibitor complexes during docking was calculated, not only the best score which indicating the matching energy was considered, but also the optimal conformation was included to achieve geometric matching and exclude unfavorable interactions. As we can see (Table 3), the results of docking were basically consistent with the rule of structure-function relationship, the substituted cinnamyl group on phenolic hydroxyl group of vanillyl moiety was helpful to enormously promote the binding affinity of the enzyme-inhibitor complexes, ester bond played important roles in interacting with the protein. As for the interaction energy, the result showed that compound **21**, **22** and **26** performed better than the original ligand tropolone and the reference drug kojic acid. Additionally, compound **21** unexpectedly exerted the best interaction with the protein, which was partly different with the result of the enzyme inhibition test. Generally, the active residues of tyrosinase including HIS 263, VAL 283, PHE 264, HIS 85, HIS 259 and ALA 286 can interact with compounds **21**, **22** and **26** in different degree (Fig. 11) [30–32], moreover, compounds **21** and **22** showed potential interaction with active copper ion in tyrosinase, which provided evidence for the result in UV–visible spectra. Compared with tropolone and kojic acid, the tests compounds had greater volume, which indicated these compounds trends to form hydrophobic effect with smaller residues in the pocket area like SER 282 and ALA 286. The residue ARG 268 was the potential key residue interacting with compounds **21** and **22** which has not been reported, the basic moiety of arginine showed electron donating property, the covalent H was easily to form H-bond with electrophilic O atom in ester group.

## 3. Conclusion

In conclusion, a series of the substituted vanillyl cinnamate analogues have been designed and synthesized as novel tyrosinase inhibitory agents and applied in anti-browning of fresh-cut apples. The results indicated that the active compounds showed tyrosinase inhibitory effect with $IC_{50}$ values range and better than kojic acid. The most promising compound **22** was proved to be potential tyrosinase inhibitor in the synthesized derivatives with the $IC_{50}$ value of 213.2 μM. Inhibition of tyrosinase activity and melanin content in B16 melanoma cells investigations indicated that compounds **21**, **22** and **26** inhibited both cellular tyrosinase activity and melanin content dose-dependently and more strongly than the reference standard arbutin. Additionally, the kinetic mechanism disclosed the competitive mode of compound **26** and the mixed-type manner of compounds **21** and **22**. Molecular docking analysis was performed to delineate the binding affinity of the ligand in the active site of target protein. Compounds **21**, **22** and **26** + 0.5% Vc showed a satisfactory effect in anti-browning of fresh-cut apples. From the above results, it could be deduced that compound **22** can serve as structural template in designing of inhibitors against tyrosinase enzyme and anti-browning agents for fresh-cut fruit, which might provide new idea for drug design.

## 4. Experimental

### 4.1. Chemistry

The chemicals and reagents were purchased from several chemical companies such as Alfa-Aesar, Macklin and *J&K* China. All reactions were monitored by TLC using silica gel plates with fluorescence F256 and UV light visualization. The mixtures were purified by flash column chromatography using silica gel (200–300 mesh). $^1$H NMR and $^{13}$C NMR spectra were obtained by Varian Gemini 2000 DMX600 MHz FT NMR spectrometers using $CDCl_3$ as a solvent and TMS as an internal standard. The chemical shifts were expressed in ppm. Mass spectral ESI measurements were executed on Agilent 6520 Accurate-mass Q-TOF LC/MS instruments. The spectra were performed in the positive ion mode at a declustering potential of 4000 V. Melting points were determined in a WRS-1B apparatus and are uncorrected.

#### 4.1.1. Synthesis of compounds *1–8* and *19–26*

General experimental procedure for the synthesis of vanillyl cinnamate derivatives (**1–8** and **19–26**): a mixture containing substituted cinnamic acids (4.0 mmol, 1.0 equiv.), 1-(3-Dimethylaminopropyl)- 3-ethylcarbodiimide hydrochloride (EDCI, 4.0 mmol, 1.0equiv.), 4-(dimethylamino)-pyridin (DMAP, 1.0 mmol, 0.25 equiv.) and vanillyl alcohol or 4-hydroxybenzyl alcohol (1.5 mmol, 0.375 equiv.) in the

**Table 3**
Measured results of binding affinity of the enzyme-inhibitor complexes for docking.

| Com. | CDOCKER interaction energy (Kcal/mol) | Key interactions |
|---|---|---|
| **Tropolone** | −41.46 | HIS 263 (pi-pi stacked), VAL 283 (pi-alkyl), CU 401 (van der Waals), PHE 264 (van der Waals), HIS 85 (van der Waals), HIS 259 (pi-donor H-bond) |
| **Kojic acid** | −32.23 | CU 401 (metal-acceptor), CU 400 (metal-acceptor), ASN260 (H-bond), HIS 263 (pi-pi stacked), VAL 283 (pi-alkyl), ALA 286 (pi-alkyl), HIS 259 (pi-donor H-bond), HIS 85 (pi-donor H-bond), HIS 296 (van der Waals) |
| **21** | −53.21 | CU 401 (metal-acceptor), CU 400 (van der Waals), ARG 268 (H-bond), HIS 263(pi-pi stacked), ASN 260 (pi-long pair), VAL 283 (pi-alkyl), ALA 286 (van der Waals), HIS 259 (pi-donor H-bond) HIS 85 (van der Waals) |
| **22** | −46.23 | CU 401 (van der Waals), ARG 268 (H-bond), HIS 263 (van der Waals), VAL 283 (pi-alkyl), SER 282 (pi-pi stacked), ALA 286 (van der Waals), HIS 85 (van der Waals), HIS 259 (van der Waals) |
| **26** | −44.53 | VAL 283 (H-bond), HIS 244 (H-bond), HIS 263 (van der Waals), PHE 264 (pi-pi stacked), ALA 286 (van der Waals), HIS 85 (van der Waals), HIS 259 (van der Waals) |

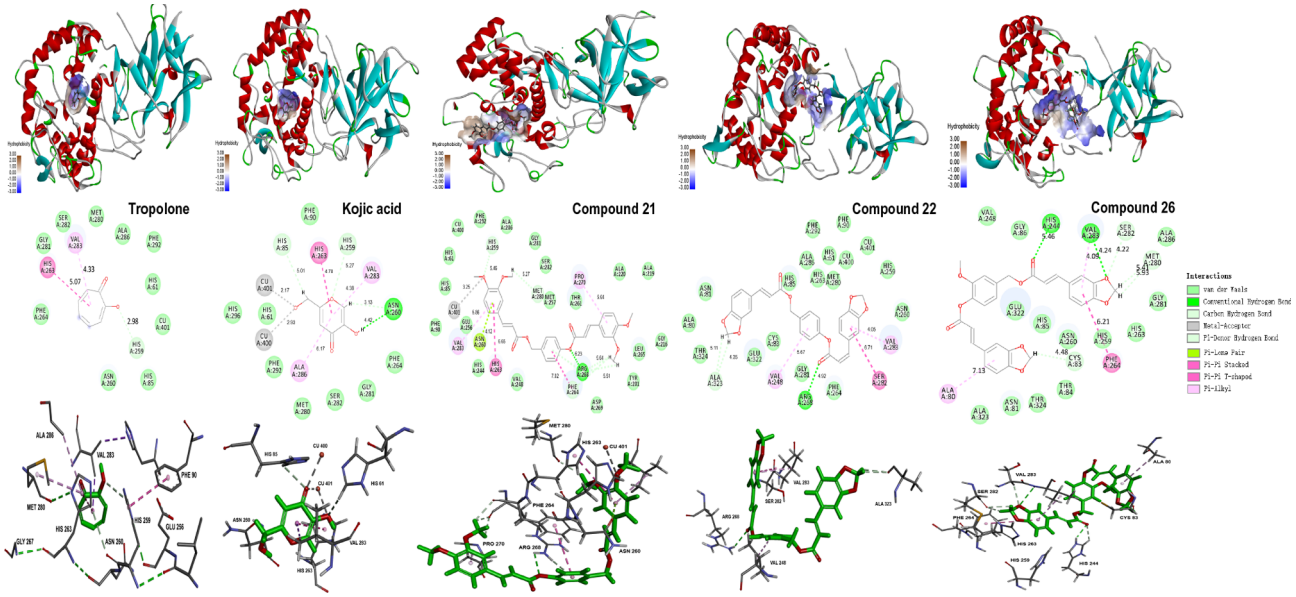


**Fig. 11.** Ligand-protein interactions of tropolone, kojic acid, active compounds **21**, **22** and **26** with the active site of mushroom tyrosinase (2Y9X) accomplished by Discovery Studio 2019 The upward side horizontal pictures show the3D docking of ligands in the active binding pocket with the hydrophobic effect area displayed. The medium row of pictures shows the 2D interaction pattern between the ligands and protein. The bottom of the figure represents the important interactions between the ligand atoms and the amino acid residues of the protein.

presence of anhydrous dichloromethane (30 mL) was thoroughly stirred at room temperature for 6–10 h till the completion of reaction. The obtained product was extracted with sodium bicarbonate water solution and diluted hydrochloric acid. The organic layer was dried over anhydrous sodium sulphate and evaporated to dryness to give the crude product. The obtained residue was purified by silica gel chromatography using petroleum ether/ethyl acetate (6:1, v:v) as original eluent to give the pure compounds **1–8** and **21–26** (Scheme 1).

### 4.1.2. Synthesis compounds *9–18*

Excess $K_2CO_3$ and a small amount of KI as the catalyst were added to a solution of the vanillin or 4-hydroxy benzaldehy (20 mmol, 1.0 equiv.) in dimethyl formamide (80 mL). After stirring for 30 min, 3-methyl-butenyl bromide or 2,3,4,6-*O*-tetraacetyl-*α*-D-glucopyranosyl bromide (22 mmol, 1.1 equiv.) was added and the resulting mixture was stirred at 65 °C for 3–6 h. After completion of the reaction, the solid was filtered, and the solution was concentrated in vacuo. The crude product was purified by chromatography on silica gel using petroleum ether/ethyl acetate (5:1, v:v) as original eluent to give the etherification intermediates. Then the substituted hydroxy aldehydes were reduced by sodium borohydride to give corresponding alcohols, and subsequently the alcohols were used to esterification with substituted cinnamic acids to give compounds **9–18** using EDCI-DMAP as activation system.

All titled compounds **1–26** were successfully synthesized using the synthetic protocols presented in Scheme 1. Identification of compounds **1–26** is listed, the identification data of some compounds can be found in our previously published literature [33]:

*4-hydroxybenzyl cinnamate **(1)*** White solid. m.p. 119–122 °C. Yield: 85%; $R_f$ = 0.5 (Hexane/EtOAc = 4:1, v/v); $^1$H NMR (600 MHz, $CDCl_3$) $\delta$ ppm: 7.88 (d, $J$ = 16.0 Hz, 1H), 7.60 (dd, $J$ = 6.7, 3.0 Hz, 2H), 7.45–7.39 (m, 5H), 7.17 (d, $J$ = 8.3 Hz, 2H), 6.64 (d, $J$ = 16.0 Hz, 1H), 4.72 (d, $J$ = 5.3 Hz, 2H); $^{13}$C NMR (151 MHz, $CDCl_3$) $\delta$ ppm: 165.66, 150.45, 146.91, 130.96, 129.23, 128.53, 128.33, 121.98, 117.42, 65.07.; HRMS(ESI) *m/z* calcd for $C_{16}H_{14}O_3$ ($[M+H]^+$): 255.1016; found: 255.1053.

*4-hydroxybenzyl (E)-3-(3,4,5-trimethoxyphenyl)acrylate **(2)***, data can be found in reference [33].

*4-hydroxybenzyl (E)-3-(3,4-dimethoxyphenyl)acrylate **(3)*** White solid. m.p. 133–135 °C. Yield: 73%; $R_f$ = 0.4 (Hexane/EtOAc = 1:1,v/v); $^1$H NMR (600 MHz, $CDCl_3$) $\delta$ ppm: 7.81 (d, $J$ = 15.9 Hz, 1H), 7.41 (d, $J$ = 8.1 Hz, 2H), 7.19–7.11 (m, 4H), 6.90 (d, $J$ = 8.3 Hz, 1H), 6.50 (d, $J$ = 15.9 Hz, 1H), 4.70 (s, 2H), 3.93 (s, 6H);$^{13}$C NMR (151 MHz, $CDCl_3$) $\delta$ ppm: 165.91, 151.73, 149.50, 146.82, 138.59, 128.30, 127.34, 123.25, 121.98, 114.98, 111.29, 109.97, 65.03, 56.22, 56.13; HRMS(ESI) *m/z* calcd for $C_{18}H_{18}O_5$ ($[M+Na]^+$): 315.1227; found: 315.1248.

*4-hydroxybenzyl (E)-3-(benzo[d][1,3]dioxol-5-yl)acrylate **(4)*** White solid. m.p. 133–137 °C. Yield: 78%; $R_f$ = 0.6 (Hexane/EtOAc = 3:1, v/v); $^1$H NMR (600 MHz, $CDCl_3$) $\delta$ ppm: 7.77 (d, $J$ = 15.9 Hz, 1H), 7.41 (d, $J$ = 8.1 Hz, 2H), 7.15 (d, $J$ = 8.2 Hz, 2H), 7.11–7.00 (m, 2H), 6.87–6.80 (m, 1H), 6.45 (d, $J$ = 15.9 Hz, 1H), 6.03 (s, 2H), 4.71 (s, 2H);$^{13}$C NMR (151 MHz, $CDCl_3$) $\delta$ ppm: 165.85, 150.50, 148.68, 146.60, 138.56, 128.81, 128.32, 125.15, 122.00, 115.24, 108.87, 106.83, 101.89, 65.08; HRMS(ESI) *m/z* calcd for $C_{17}H_{14}O_5$ $[M+H]^+$): 299.0914; found: 299.0919.

*4-hydroxy-3-methoxybenzyl cinnamate **(5)*** White solid. m.p. 130–134 °C. Yield: 75%; $R_f$ = 0.6 (Hexane/EtOAc = 2:1, v/v); $^1$H NMR (600 MHz, $CDCl_3$) $\delta$ ppm: 7.88 (d, $J$ = 16.0 Hz, 1H), 7.59 (dd, $J$ = 6.5, 3.0 Hz, 2H), 7.46–7.37 (m, 3H), 7.14–7.03 (m, 2H), 6.95 (d, $J$ = 8.0 Hz, 1H), 6.67 (d, $J$ = 16.0 Hz, 1H), 4.70 (s, 2H), 3.85 (s, 4H);$^{13}$C NMR (151 MHz, $CDCl_3$) $\delta$ ppm: 165.28, 146.87, 140.10, 134.45, 130.85, 129.17, 128.52, 123.07, 119.23, 117.13, 111.30, 65.31, 56.16; HRMS (ESI) *m/z* calcd for $C_{17}H_{16}O_4$ $[M+H]^+$): 307.0941; found: 307.0956.

*4-hydroxy-3-methoxybenzyl (E)-3-(3,4,5-trimethoxyphenyl)acrylate **(6)***, data can be found in reference [33].

*4-hydroxy-3-methoxybenzyl (E)-3-(3,4-dimethoxyphenyl)acrylate **(7)*** White solid. m.p. 146–149 °C. Yield: 74%; $R_f$ = 0.4 (Hexane/EtOAc = 2:1,v/v); $^1$H NMR (600 MHz, $CDCl_3$) $\delta$ ppm: 7.82 (d, $J$ = 15.8 Hz, 1H), 7.17 (dd, $J$ = 8.2, 1.9 Hz, 1H), 7.12 (d, $J$ = 1.9 Hz, 1H), 7.10–7.05 (m, 2H), 6.97–6.94 (m, 1H), 6.89 (d, $J$ = 8.2 Hz, 1H), 6.55 (d, $J$ = 15.9 Hz, 1H), 4.70 (d, $J$ = 5.4 Hz, 2H), 3.93 (d, $J$ = 2.6 Hz, 6H), 3.86 (d, $J$ = 1.8 Hz, 3H); $^{13}$C NMR (151 MHz, $CDCl_3$) $\delta$ ppm: 165.52, 151.64, 149.46, 146.80, 140.01, 139.39, 127.45, 123.28, 123.13, 119.24, 114.73, 111.28, 111.26, 109.91, 65.35, 56.21, 56.12; HRMS(ESI) *m/z* calcd for$C_{19}H_{20}O_6$ $[M+H]^+$): 345.1333; found: 345.1355.

*4-hydroxy-3-methoxybenzyl (E)-3-(benzo[d][1,3]dioxol-5-yl)acrylate*

***(8)*** White solid. m.p. 150–156 °C. Yield: 71%; $R_f$ = 0.7 (Hexane/EtOAc = 4:1, v/v); $^1$H NMR (600 MHz, $CDCl_3$) $\delta$ ppm: 7.78 (d, $J$ = 15.9 Hz, 1H), 7.11–7.04 (m, 5H), 6.95 (dd, $J$ = 8.0, 1.8 Hz, 1H), 6.84 (d, $J$ = 8.0 Hz, 1H), 6.49 (d, $J$ = 15.9 Hz, 1H), 6.03 (s, 2H), 4.70 (d, $J$ = 4.7 Hz, 2H), 3.85 (s, 3H);$^{13}$C NMR (151 MHz, $CDCl_3$) $\delta$ 165.44, 151.60, 150.15, 148.63, 146.56, 140.01, 139.39, 128.92, 125.10, 123.12, 119.24, 115.00, 111.30, 108.83, 106.86, 101.85, 65.36, 56.17; HRMS(ESI) *m/z* calcd for$C_{18}H_{16}O_6$ ($[M+Na]^+$): 351.0839; found: 351.0851.

*4-((3-methylbut-2-en-1-yl)oxy)benzyl cinnamate* ***(9)*** Yellow liquid. Yield: 74%; Rf = 0.7 (Hexane/EtOAc = 5:1, v/v);$^1$H NMR (600 MHz, Chloroform-*d*) $\delta$ ppm: 7.72 (d, $J$ = 16.0 Hz, 1H), 7.51 (dd, $J$ = 6.5, 3.1 Hz, 2H), 7.41–7.34 (m, 5H), 6.93 (d, $J$ = 8.3 Hz, 2H), 6.47 (d, $J$ = 15.9 Hz, 1H), 5.50 (t, $J$ = 6.9 Hz, 1H), 5.19 (s, 2H), 4.53 (d, $J$ = 6.8 Hz, 2H), 1.81 (s, 3H), 1.75 (s, 3H).;$^{13}$C NMR (151 MHz, cdcl$_3$) $\delta$ ppm: 167.06, 159.17, 145.18, 138.49, 134.60, 130.32, 129.07, 128.27, 119.76, 118.25, 114.91, 66.44, 64.99, 26.03, 18.40.; HRMS(ESI) *m/z* calcd for$C_{21}H_{22}O_3$ ($[M+Na]^+$): 345.1416; found: 345.1447.

*4-((3-methylbut-2-en-1-yl)oxy)benzyl (E)-3-(3,4,5-trimethoxyphenyl) acrylate* ***(10)***, data can be found in reference [33].

*4-((3-methylbut-2-en-1-yl)oxy)benzyl (E)-3-(3,4-dimethoxyphenyl)acrylate* ***(11)***Pale yellow solid. m.p. 56–60 °C. Yield: 61%; $R_f$ = 0.6 (Hexane/EtOAc = 5:1, v/v);$^1$H NMR (600 MHz, $CDCl_3$) $\delta$ ppm: 7.65 (d, $J$ = 15.9 Hz, 1H), 7.37–7.33 (m, 2H), 7.09 (dd, $J$ = 8.3, 2.0 Hz, 1H), 7.03 (d, $J$ = 2.0 Hz, 1H), 6.93–6.90 (m, 2H), 6.85 (d, $J$ = 8.3 Hz, 1H), 6.34 (d, $J$ = 15.9 Hz, 1H), 5.52–5.47 (m, 1H), 5.17 (s, 2H), 4.52 (d, $J$ = 6.7 Hz, 2H), 3.91 (s, 4H), 3.89 (s, 3H), 1.80 (s, 3H), 1.74 (s, 2H);$^{13}$C NMR (151 MHz, $CDCl_3$) $\delta$ ppm: 167.30, 159.15, 151.33, 149.39, 145.09, 138.53, 130.32, 128.35, 127.60, 122.85, 119.75, 115.94, 114.92, 111.21, 109.76, 66.34, 65.01, 56.06, 26.04, 18.41; HRMS(ESI) *m/z* calcd for $C_{23}H_{26}O_5$ ($[M+Na]^+$): 405.1672; found: 405.1614.

*4-((3-methylbut-2-en-1-yl)oxy)benzyl (E)-3-(benzo[d]*[1,3]*dioxol-5-yl)acrylate* ***(12)*** Pale yellow solid. m.p. 81–83 °C. Yield: 69%; $R_f$ = 0.7 (Hexane/EtOAc = 5:1, v/v); $^1$H NMR (600 MHz, $CDCl_3$) $\delta$ ppm: 7.61 (d, $J$ = 15.9 Hz, 1H), 7.34 (d, $J$ = 8.5 Hz, 2H), 7.03–6.97 (m, 2H), 6.94–6.90 (m, 2H), 6.80 (d, $J$ = 8.0 Hz, 1H), 6.28 (d, $J$ = 15.9 Hz, 1H), 5.99 (s, 2H), 5.53–5.46 (m, 1H), 5.17 (s, 2H), 4.52 (d, $J$ = 6.7 Hz, 2H), 1.80 (s, 3H), 1.75 (s, 3H);$^{13}$C NMR (151 MHz, $CDCl_3$) $\delta$ ppm: 167.27, 159.14, 149.82, 148.53, 144.89, 138.55, 130.32, 129.05, 128.34, 124.66, 119.75, 116.18, 114.91, 108.75, 106.70, 101.75, 66.35, 65.00, 26.05, 18.42; HRMS(ESI) *m/z* calcd for $C_{22}H_{22}O_5$ ($[M+Na]^+$): 389.1365; found: 389.1357.

*3-methoxy-4-((3-methylbut-2-en-1-yl)oxy)benzyl cinnamate* ***(13)***, data can be found in reference [33].

*3-methoxy-4-((3-methylbut-2-en-1-yl)oxy)benzyl (E)-3-(3,4,5-trimethoxyphenyl)acrylate* ***(14)***, data can be found in reference [33].

*2-(acetoxymethyl)-6-(4-((cinnamoyloxy)methyl)phenoxy)tetrahydro-2H-pyran-3,4,5-triyl triacetate* ***(15)*** Pale yellow solid. m.p. 108–110 °C. Yield: 67%; $R_f$ = 0.5 (Hexane/EtOAc = 1:1, v/v); $^1$H NMR (600 MHz, $CDCl_3$) $\delta$ ppm: 7.71 (d, $J$ = 16.0 Hz, 1H), 7.51 (dd, $J$ = 6.7, 3.0 Hz, 2H), 7.40–7.35 (m, 5H), 7.00 (d, $J$ = 8.3 Hz, 2H), 6.46 (d, $J$ = 16.0 Hz, 1H), 5.33–5.25 (m, 2H), 5.18 (d, $J$ = 15.1 Hz, 3H), 5.09 (d, $J$ = 7.1 Hz, 1H), 4.29 (dd, $J$ = 12.3, 5.3 Hz, 1H), 4.17 (dd, $J$ = 12.3, 2.4 Hz, 1H), 3.91–3.80 (m, 1H), 2.08 (s, 3H), 2.07–2.03 (m, 10*H*); $^{13}$C NMR (151 MHz, $CDCl_3$) $\delta$ ppm: 170.79, 170.46, 169.61, 169.51, 166.99, 157.02, 145.47, 134.51, 131.32, 130.61, 130.24, 129.12, 128.31, 117.99, 117.25, 99.26, 72.91, 72.29, 71.36, 68.48, 66.05, 62.15, 32.14, 29.92, 29.88, 20.92, 20.85, 20.84, 20.81; HRMS(ESI) *m/z* calcd for$C_{30}H_{32}O_{12}$ ($[M+Na]^+$): 607.1786; found: 607.1800.

*(2R,3R,4S,5R,6S)-2-(acetoxymethyl)-6-(4-((((E)-3-(3,4,5-trimethoxyphenyl)acryloyl)oxy)methyl)phenoxy)tetrahydro-2H-pyran-3,4,5-triyl triacetate****(16)***, data can be found in reference [33].

*(E)-2-(acetoxymethyl)-6-(4-(((3-(3,4-dimethoxyphenyl)acryloyl)oxy) methyl)phenoxy)tetrahydro-2H-pyran-3,4,5-triyl triacetate* ***(17)*** White solid. m.p. 137–140 °C. Yield: 61%; $R_f$ = 0.4 (Hexane/EtOAc = 1:1, v/v); $^1$H NMR (600 MHz, $CDCl_3$) $\delta$ ppm: 7.65 (d, $J$ = 15.9 Hz, 1H), 7.39–7.34 (m, 2H), 7.09 (dd, $J$ = 8.3, 2.0 Hz, 1H), 7.06–6.98 (m, 3H), 6.86 (d, $J$ = 8.3 Hz, 1H), 6.33 (d, $J$ = 15.8 Hz, 1H), 5.32–5.25 (m, 2H), 5.18 (d, $J$ = 9.7 Hz, 3H), 5.08 (d, $J$ = 7.5 Hz, 1H), 4.29 (dd, $J$ = 12.3, 5.3 Hz, 1H), 4.19–4.09 (m, 2H), 3.90 (d, $J$ = 7.0 Hz, 6H), 3.86 (dd, $J$ = 10.1, 5.3, 2.4 Hz, 1H), 2.08 (s, 3H), 2.06–2.03 (m, 9H);$^{13}$C NMR (151 MHz, $CDCl_3$) $\delta$ ppm: 170.78, 170.46, 169.60, 169.50, 167.20, 157.01, 151.44, 149.44, 145.37, 131.45, 130.23, 117.27, 115.67, 111.25, 109.80, 99.28, 72.92, 72.30, 71.37, 68.49, 65.94, 62.15, 56.20, 56.10, 20.86, 20.82; HRMS(ESI) *m/z* calcd for$C_{32}H_{36}O_{14}$ ($[M+Na]^+$): 667.1997; found: 667.2010.

*(E)-2-(acetoxymethyl)-6-(4-(((3-(benzo[d]*[1,3]*dioxol-5-yl)acryloyl) oxy)methyl)phenoxy)tetrahydro-2H-pyran-3,4,5-triyl triacetate* ***(18)*** Pale yellow solid. m.p. 110–113 °C. Yield: 52%; $R_f$ = 0.5 (Hexane/EtOAc = 4:1, v/v); $^1$H NMR (600 MHz, $CDCl_3$) $\delta$ ppm: 7.58 (d, $J$ = 15.9 Hz, 1H), 6.76 (s, 2H), 6.37 (d, $J$ = 15.8 Hz, 1H), 5.02 (dt, $J$ = 9.9, 2.8 Hz, 1H), 4.00 (dt, $J$ = 10.0, 2.7 Hz, 1H), 3.90 (s, 6H), 3.88 (s, 3H), 2.46–2.39 (m, 1H), 2.27 (ddt, $J$ = 15.0, 8.1, 2.4 Hz, 1H), 2.06 (ddd, $J$ = 13.3, 9.4, 4.4 Hz, 1H), 1.89 (ddd, $J$ = 15.2, 10.1, 4.5 Hz, 1H), 1.71 (t, $J$ = 4.7 Hz, 2H), 1.62 (s, 1H), 0.87–0.83 (m, 9H); $^{13}$C NMR (151 MHz, $CDCl_3$) $\delta$ ppm: 170.78, 170.45, 169.60, 169.50, 167.15, 156.99, 149.91, 148.56, 145.15, 131.41, 130.21, 128.93, 124.75, 117.23, 115.88, 108.77, 106.67, 101.79, 99.26, 72.90, 72.28, 71.34, 68.46, 65.93, 62.14, 60.61, 29.91, 20.92, 20.85, 20.84, 20.81; HRMS (ESI) *m/z* calcd for$C_{31}H_{32}O_{14}$ ($[M+Na]^+$): 651.1684; found: 651.1689.

*4-(cinnamoyloxy)benzyl cinnamate* ***(19)*** White solid. m.p. 107–110 °C. Yield: 64%; $R_f$ = 0.7 (Hexane/EtOAc = 3:1, v/v); $^1$H NMR (600 MHz, $CDCl_3$) $\delta$ ppm: 7.88 (d, $J$ = 16.0 Hz, 1H), 7.74 (d, $J$ = 16.0 Hz, 1H), 7.60 (dd, $J$ = 6.7, 3.0 Hz, 2H), 7.53 (dd, $J$ = 6.7, 3.1 Hz, 2H), 7.47 (d, $J$ = 8.1 Hz, 2H), 7.45–7.42 (m, 3H), 7.41–7.38 (m, 3H), 7.20 (d, $J$ = 8.4 Hz, 2H), 6.64 (d, $J$ = 16.0 Hz, 1H), 6.49 (d, $J$ = 16.0 Hz, 1H), 5.26 (s, 2H).; $^{13}$C NMR (151 MHz, $CDCl_3$) $\delta$ ppm: 166.95, 165.53, 150.92, 146.99, 145.53, 130.98, 130.60, 129.79, 129.23, 129.12, 128.54, 128.35, 122.04, 118.00, 117.36, 65.97.; HRMS (ESI) *m/z* calcd for$C_{25}H_{20}O_4$ ($[M+Na]^+$): 407.1254; found: 407.1266.

*4-(((E)-3-(3,4,5-trimethoxyphenyl)acryloyl)oxy)benzyl (E)-3-(3,4,5-trimethoxyphenyl)acrylate* ***(20)*** White solid. m.p. 88–91 °C. Yield: 53%; $R_f$ = 0.7 (Hexane/EtOAc = 2:1, v/v); $^1$H NMR (600 MHz, $CDCl_3$) $\delta$ ppm: 7.79 (d, $J$ = 15.9 Hz, 1H), 7.64 (d, $J$ = 15.9 Hz, 1H), 7.50–7.43 (m, 2H), 7.22–7.18 (m, 2H), 6.82 (s, 2H), 6.76 (s, 2H), 6.54 (d, $J$ = 15.9 Hz, 1H), 6.39 (d, $J$ = 15.9 Hz, 1H), 5.25 (s, 2H), 3.90 (dd, $J$ = 14.7, 3.1 Hz, 18H); $^{13}$C NMR (151 MHz, $CDCl_3$) $\delta$ ppm: 166.85, 165.51, 153.72, 153.64, 150.93, 147.29, 145.79, 140.79, 133.82, 130.11, 130.01, 129.76, 121.96, 116.49, 105.90, 105.63, 105.54, 105.32, 65.98, 61.20, 56.38; HRMS(ESI) *m/z* calcd for$C_{31}H_{32}O_{10}$ ($[M+Na]^+$): 587.1888; found: 587.1897.

*4-(((E)-3-(3,4-dimethoxyphenyl)acryloyl)oxy)benzyl (E)-3-(3,4-dimethoxyphenyl)acrylate* ***(21)*** White solid. m.p. 117–120 °C. Yield: 59%; $R_f$ = 0.7 (Hexane/EtOAc = 2:1, v/v); $^1$H NMR (600 MHz, $CDCl_3$) $\delta$ ppm: 7.82 (d, $J$ = 15.9 Hz, 1H), 7.67 (d, $J$ = 15.9 Hz, 1H), 7.21–7.01 (m, 7H), 6.88 (dd, $J$ = 20.3, 8.3 Hz, 2H), 6.50 (d, $J$ = 15.8 Hz, 1H), 6.35 (d, $J$ = 15.9 Hz, 1H), 5.24 (s, 2H), 3.93 (d, $J$ = 1.7 Hz, 6H), 3.91 (d, $J$ = 1.9 Hz, 7H); $^{13}$C NMR (151 MHz, cdcl$_3$) $\delta$ ppm: 167.18, 165.79, 151.41, 150.97, 149.41, 146.92, 145.42, 133.84, 129.76, 127.52, 127.31, 123.28, 122.91, 122.05, 115.65, 114.90, 111.30, 111.24, 109.97, 65.88, 56.22; HRMS(ESI) *m/z* calcd for $C_{29}H_{28}O_8$ ($[M+Na]^+$): 527.1676; found: 527.1671.

*4-(((E)-3-(benzo[d]*[1,3]*dioxol-5-yl)acryloyl)oxy)benzyl (E)-3-(benzo [d]*[1,3]*dioxol-5-yl)acrylate* ***(22)*** White solid. m.p. 133–137 °C. Yield: 51%; $R_f$ = 0.7 (Hexane/EtOAc = 3:1, v/v); $^1$H NMR (600 MHz, $CDCl_3$) $\delta$ ppm: 7.77 (d, $J$ = 15.9 Hz, 1H), 7.63 (d, $J$ = 15.9 Hz, 1H), 7.45 (d, $J$ = 8.1 Hz, 2H), 7.18 (d, $J$ = 8.1 Hz, 2H), 7.13–7.06 (m, 2H), 7.05–6.98 (m, 2H), 6.83 (dd, $J$ = 20.7, 8.0 Hz, 2H), 6.45 (d, $J$ = 15.9 Hz, 1H), 6.30 (d, $J$ = 15.9 Hz, 1H), 6.03 (s, 2H), 6.00 (s, 2H), 5.24 (s, 2H); $^{13}$C NMR (151 MHz, $CDCl_3$) $\delta$ ppm: 167.14, 165.72, 150.93, 150.25, 149.90, 148.56, 146.67, 145.20, 133.82, 129.73, 128.98, 128.78, 125.17, 124.77, 122.03, 115.89, 115.17, 108.86, 108.76, 106.81,

106.74, 101.88, 101.77, 65.88; HRMS(ESI) *m/z* calcd for$C_{27}H_{20}O_8$ ([M + Na]$^+$): 495.1056; found: 495.1019.

*4-(cinnamoyloxy)-3-methoxybenzyl cinnamate* ***(23)*** White solid. m.p. 166–169 °C. Yield: 58%; $R_f$ = 0.7 (Hexane/EtOAc = 4:1, v/v); $^1$H NMR (600 MHz, $CDCl_3$) $\delta$ ppm: 7.89 (d, $J$ = 16.0 Hz, 1H), 7.75 (d, $J$ = 16.0 Hz, 1H), 7.62–7.58 (m, 2H), 7.56–7.51 (m, 2H), 7.44–7.41 (m, 3H), 7.41–7.38 (m, 3H), 7.13 (d, $J$ = 8.0 Hz, 1H), 7.07–7.03 (m, 2H), 6.68 (d, $J$ = 16.0 Hz, 1H), 6.50 (d, $J$ = 16.0 Hz, 1H), 5.25 (s, 2H), 3.87 (s, 3H); $^{13}$C NMR (151 MHz, $CDCl_3$) $\delta$ ppm: 166.96, 165.12, 151.52, 146.92, 145.58, 139.94, 135.12, 134.45, 130.87, 130.62, 129.18, 128.53, 128.36, 123.21, 121.02, 117.98, 117.11, 112.81, 66.30, 56.23; HRMS(ESI) *m/z* calcd for$C_{26}H_{22}O_5$ ([M + Na]$^+$): 437.1359; found: 437.1368.

*2-methoxy-4-((((E)-3-(3,4,5-trimethoxyphenyl)acryloyl)oxy)methyl) phenyl (E)-3-(3,4,5-trimethoxyphenyl)acrylate* ***(24)*** White solid. m.p. 173–176 °C. Yield: 57%; $R_f$ = 0.6 (Hexane/EtOAc = 2:1, v/v); $^1$H NMR (600 MHz, $CDCl_3$) $\delta$ ppm: 8.00 (d, $J$ = 15.9 Hz, 1H), 7.86 (d, $J$ = 15.9 Hz, 1H), 7.47 (s, 1H), 7.34 (d, $J$ = 7.8 Hz, 1H), 7.14–7.01 (m, 3H), 6.97 (s, 2H), 6.79 (d, $J$ = 15.9 Hz, 1H), 6.61 (d, $J$ = 15.9 Hz, 1H), 5.44 (s, 2H), 4.11–4.08 (m, 21H); $^{13}$C NMR (151 MHz, $CDCl_3$) $\delta$ ppm: 166.89, 165.13, 153.66, 151.51, 146.94, 145.54, 140.69, 139.96, 135.10, 129.89, 123.25, 121.14, 117.19, 116.26, 112.91, 105.71, 66.36, 61.20, 56.39, 56.25; HRMS(ESI) *m/z* calcd for$C_{32}H_{34}O_{11}$ ([M + Na]$^+$): 617.1993; found: 617.1948.

*4-(((E)-3-(3,4-dimethoxyphenyl)acryloyl)oxy)-3-methoxybenzyl (E)-3-(3,4-dimethoxyphenyl)acrylate* ***(25)*** White solid. mp 165–169 °C. Yield: 55%; $R_f$ = 0.6 (Hexane/EtOAc = 2:1, v/v); $^1$H NMR (600 MHz, $CDCl_3$) $\delta$ ppm: 7.82 (d, $J$ = 15.9 Hz, 1H), 7.68 (d, $J$ = 15.9 Hz, 1H), 7.17 (dd, $J$ = 8.4, 2.0 Hz, 1H), 7.13–7.10 (m, 3H), 7.07–7.02 (m, 3H), 6.93–6.83 (m, 3H), 6.55 (d, $J$ = 15.9 Hz, 1H), 6.37 (d, $J$ = 15.9 Hz, 1H), 5.23 (s, 2H), 3.93 (s, 4H), 3.91 (d, $J$ = 1.6 Hz, 7H), 3.87 (s, 3H); $^{13}$C NMR (151 MHz, $CDCl_3$) $\delta$ ppm: 167.18, 165.39, 151.66, 149.47, 149.42, 146.88, 145.47, 139.98, 135.13, 127.51, 123.30, 123.26, 122.92, 121.05, 115.63, 114.67, 112.82, 111.25, 111.24, 109.90, 109.85, 66.23, 56.23, 56.21, 56.19, 56.12, 56.10; HRMS(ESI) *m/z* calcd for$C_{30}H_{30}O_9$ ([M + Na]$^+$): 557.1782; found: 557.1717.

*4-(((E)-3-(benzo[d][1,3]dioxol-5-yl)acryloyl)oxy)-3-methoxybenzyl (E)-3-(benzo[d][1,3]dioxol-5-yl)acrylate* ***(26)*** White solid. mp 186–190 °C. Yield: 65%; $R_f$ = 0.7 (Hexane/EtOAc = 5:1, v/v); $^1$H NMR (600 MHz, $CDCl_3$) $\delta$ ppm: 7.78 (d, $J$ = 15.9 Hz, 1H), 7.64 (d, $J$ = 15.9 Hz, 1H), 7.15–7.00 (m, 7H), 6.83 (dd, $J$ = 14.5, 8.0 Hz, 2H), 6.49 (d, $J$ = 15.8 Hz, 1H), 6.32 (d, $J$ = 15.9 Hz, 1H), 6.02 (d, $J$ = 13.2 Hz, 4H), 5.22 (s, 2H), 3.86 (s, 3H).; $^{13}$C NMR (151 MHz, $CDCl_3$) $\delta$ ppm: 167.14, 165.31, 151.53, 146.62, 145.25, 139.95, 135.13, 128.98, 125.11, 124.79, 123.22, 121.00, 115.88, 114.96, 112.78, 108.78, 106.86, 106.74, 101.85, 66.21, 56.22; HRMS(ESI) *m/z* calcd for $C_{28}H_{22}O_9$ ([M + Na]$^+$): 525.1156; found: 525.1150.

### 4.2. Biological activity

#### 4.2.1. Tyrosinase inhibition assay

The measurement of tyrosinase (EC 1.14.18.1) inhibition was possessed according to the method of Saeed [1] with minor modifications. Briefly, 30 μL of mushroom tyrosinase (24 U/mL) and 70 μL of the inhibitor solution (1 mg/mL) were placed in the wells of a 96-well micro plate. After pre-incubation for 10 min at room temperature, 110 μL of L-Dopa (1 mM) was added. After that 40 μL of phosphate buffer (20 mM, pH 6.8) was add into each well to a final volume at 250 μL and the assay plate was further incubated at 35 °C for 12 min. Afterward the absorbance of dopachrome was measured at 475 nm using a micro plate reader (INFINITE 200 PRO, TECAN, Tunable). Kojic acid (0.125, 0.25, 0.5, 1, 2 and 4 mM) was used as a reference inhibitor and phosphate buffer was used as a negative control. The amount of inhibition by the test compounds was expressed as the percentage (%) in the preliminary screening. Then 50% inhibiting concentration ($IC_{50}$) for active compounds was preliminary screen. Each concentration was determined in three independent experiments.

The inhibition ratio of tyrosinase was calculated according to the result from following formula:

$$\text{Inhibition}(\%) = [(A_{sample} - A_{blank})/A_{control}] \times 100\%$$

$A_{sample}$ denotes the $OD_{475}$ absorbance of test compound and $A_{blank}$ is the $OD_{475}$ absorbance for the blank. $A_{control}$ represents the $OD_{475}$ absorbance of control.

#### 4.2.2. Cytotoxicity

Normal liver cell L02 and B16 melanoma cell line obtained from Xi'an jiaotong University, China, were cultured at 37 °C under a 5% $CO_2$ atmosphere and was used to determine the cytotoxicity of compounds **21, 22** and **26**. The L02 cells (10000 cells/well) and B16 cells (50000 cells/well) were seeded in Dulbecco's modified Eagle's medium (DMEM) containing 100 IU/mL penicillin, and 100 μg/mL streptomycin, supplemented with 10% FBS (GIBCO, Invitrogen Corporation, Grand Island, NY, USA), under 5% $CO_2$ humidified atmosphere at 37 °C. The cell viability assay was evaluated by the conversion of Cell Counting Kit-8 (CCK-8) to a purple formazan precipitate as previously described. After 24 h, the various concentrations of compounds were subsequently added and incubated for 24 h. The survival rate was calculated from plotted results using cells untreated by test compounds as reference [3,34,35].

$$\text{Cellviability}(\%) = [(A_{sample} - A_{blank})/(A_{control} - A_{blank})] \times 100$$

$A_{sample}$ denotes the $OD_{450}$ absorbance of test compound and $A_{blank}$ is the $OD_{450}$ absorbance for the blank. $A_{control}$ represents the $OD_{450}$ absorbance of control.

#### 4.2.3. Determination of cellular tyrosinase activity

To determine the cellular tyrosinase activity, the B16 melanoma cells were placed in a 24-well plate and was evaluated by quantifying the L-DOPA oxidation rate with slight modification [9,36]. Control group containing $1 \times 10^5$ cells per well, and treated group with $1 \times 10^5$ cells containing 1 μM α-MSH and various concentrations of compounds **21, 22** and **26** (25, 50, 100, and 200 μM) or arbutin (1 mM) for 48 h. The medium was removed and then 1% Triton X-100 mixed in 10 mM phosphate buffered saline was added. The mixture was frozen at −80 °C and thawed at room temperature. A freshly prepared substrate (2 mM L-DOPA) was then added to the supernatant and incubated. The absorbance of each well was subsequently read at 475 nm.

$$\text{Tyrosinaseactivity}(\%) = [(A_{sample} - A_{blank})/(A_{control} - A_{blank})] \times 100$$

$A_{sample}$ denotes the $OD_{475}$ absorbance of test compound and $A_{blank}$ is the $OD_{475}$ absorbance for the blank. $A_{control}$ represents the $OD_{475}$ absorbance of control.

#### 4.2.4. Measurement of melanin content

Melanin content assay was performed to evaluate the inhibitory effect of compounds **21, 22** and **26** (25, 50, 100, and 200 μM) on melanogenesis using the standard method with slight modification [8,9]. Briefly, the B16 melanoma cells were placed in a 24-well plate at a density of $1 \times 10^5$ cells per well. The treated group had a medium containing 2 μM α-MSH and various concentrations of compounds **21, 22** and **26** (25, 50, 100, and 200 μM) or arbutin (1 mM) for 48 h. The medium was removed, 1 N NaOH was added and boiled for 1 h at 80 °C. Melanin content were calculated by the OD at 405 nm.

$$\text{Melanincontent}(\%) = [(A_{sample} - A_{blank})/(A_{control} - A_{blank})] \times 100$$

$A_{sample}$ denotes the $OD_{405}$ absorbance of test compound and $A_{blank}$ is the $OD_{405}$ absorbance for the blank. $A_{control}$ represents the $OD_{405}$ absorbance of control.

#### 4.2.5. Kinetic analysis

The inhibition kinetics of compounds **21**, **22** and **26** on the

tyrosinase were investigated using Lineweaver-Burk plots at the wavelength in 475 nm [3]. The reaction mixture was consisted of eight different concentrations of L-DOPA (0.6–5 mM) as substrate and mushroom tyrosinase in phosphate buffer (20 mM, pH 6.8). Test samples at various concentrations (0–1 μM) were added to the reaction mixture. The measurement was performed at 475 nm.

#### 4.2.6. UV–visible spectra measurements

Several tyrosinase inhibitors that chelate the copper ions in the active site of the enzyme exhibited favorable inhibitory effect; existing literatures reported examples including kojic acid [37], 4-ethoxycinnamic acid [24] and tropolone [37]. To investigate whether the most promising compound **22** displayed its inhibitory effect by chelating the copper ions at the active site of tyrosinase, copper sulphate ($CuSO_4$) was added to the assay medium. The absorption spectra were taken (220 nm to 400 nm, 25 °C) of a 3.00 mL mixture containing 40 μM compound **22** and various concentrations of $CuSO_4$ after preincubating for 1 min. Scans of a 3 mL mixture consisting of compound **22** and tyrosinase were also taken after incubation at 25 °C for 3 min in the ultraviolet spectrophotometer (MAPAPA UV6100S, China). Differential spectra were obtained by subtracting the spectra from the corresponding spectrum of the mixture.

#### 4.2.7. Browning inhibition of compounds *21*, *22* and *26* on fresh-cut apple slices

The anti-browning activity of compounds **21**, **22** and **26** was evaluated with a help of fresh-cut apple slice model [26]. 'Fuji' apples (planted in Luochuan, Shanxi province, China) were picked up from the same batch with similar size and maturity without injuries, diseases or pests. The selected apples were washed with distilled water and cut into pieces (8 mm × 8 mm × 8 mm). The fresh-cut apple slices were treated by dipping in 100 mL test solution for 3 min and drained. Control samples were dipped in distilled water. Samples were then placed in individual polypropylene film bags (6 samples in each bag; 3 bags for each group), and stored at 4 °C for up to 48 h. Replicate samples (n = 18) were prepared for each treatment and the experiment was repeated three times. Test solutions used for the above samples including water, aqueous solutions of 0.5% Vc, 2 mM 4-hydroxybenzyl alcohol, 2 mM vanillyl alcohol, 2 mM cinnamic acid, 2 mM the test compounds, 2 mM compound **21** + 0.5% Vc, 2 mM compound **22** + 0.5% Vc, 2 mM compound **26** + 0.5% Vc. The relative extents of browning were assessed after measuring by the Commission Internationale de L'Eclairage (CIE) $L*a*b*$ color system (1976), using a WSC-S Color meter (Shanghai Precision Scientific Instrument Co., Ltd., Shanghai, China). $L*$ values represent the degree of darkness and lightness. The relative extents of browning were measured with a tristimulus reflectance colorimeter. The determinations were possessed following each treatment and at timed intervals of 6, 12, 24, 36, and 48 h thereafter.

#### 4.2.8. Statistical analysis

All experiments were performed in triplicate. An analysis of variance (ANOVA) of the data was performed using the GraphPad Prism 7 system. Data in the tables and figures were given as mean ± SD and analyzed by one-way ANOVA. Significant differences between the treatments were examined by Tukey's multiple range tests.

#### 4.2.9. Molecular modeling

The 3D crystal structure of mushroom tyrosinase (*Agaricus bisporus*) (PDB code: 2Y9X) was obtained from the Protein Data Bank (PDB). Docking experiment was possessed on tropolone, kojic acid, active compounds **21**, **22** and **26** against mushroom tyrosinase 2Y9X [38–40]. The ligand-protein interactions generated through the Flexible docking module of Discovery Studio 2019. To perform the docking experiment, input site sphere dimension values were adjusted as X = −8.87, Y = −30.74 and Z = −41.52, respectively, and the binding pocket was set according to the coordinates of original ligands with the radius of 15 Å. The active site AC3 (ASN 260, HIS 263, PHE 264, MET 280, VAL 283 and ALA 286) of 2Y9X, an important active site which interacts with the original ligand tropolone, was set to be the rotatable residues to acquire dovetail conformation. The docked complex was further assessed on CDOCKER interaction energy (Kcal/mol) value to evaluate the degree of energy matching, hydrogen and hydrophobic bond interaction pattern analysis using Discovery Studio 2019 software.

## Declaration of Competing Interest

The authors declare that they have no known competing financial interests or personal relationships that could have appeared to influence the work reported in this paper.

## Acknowledgments

This work was supported by the Changjiang Scholars and Innovative Research Team in Universities, Ministry of Education of China (IRT_15R55), the 7th Group of Hundred-Talent Program of Shaanxi Province (2015), and Natural Science Foundation of Shaanxi Province, China (Grant No. 2017JM8054).

## References

[1] A. Saeed, P.A. Mahesar, P.A. Channar, Q. Abbas, F.A. Larik, M. Hassan, H. Raza, S.Y. Seo, Synthesis, molecular docking studies of coumarinyl-pyrazolinyl substituted thiazoles as non-competitive inhibitors of mushroom tyrosinase, Bioorg. Chem. 74 (2017) 187–196.
[2] S. Genovese, F. Epifano, P. Medina, N. Caron, A. Rives, M. Poirot, S. Silvente-Poirot, S. Fiorito, Natural and semisynthetic oxyprenylated aromatic compounds as stimulators or inhibitors of melanogenesis, Bioorg. Chem. 87 (2019) 181–190.
[3] Y.H. Hu, Q.X. Chen, Y. Cui, H.J. Gao, L. Xu, X.Y. Yu, Y. Wang, C.L. Yan, Q. Wang, 4-Hydroxy cinnamic acid as mushroom preservation: anti-tyrosinase activity kinetics and application, Int. J. Biol. Macromol. 86 (2016) 489–495.
[4] S.Y. Seo, V.K. Sharma, N. Sharma, Mushroom tyrosinase: recent prospects, J. Agr. Food Chem. 51 (2003) 2837–2853.
[5] Z.D. He, C.F. Qiao, Q.B. Han, C.L. Cheng, H.X. Xu, R.W. Jiang, P.P.H. But, P.C. Shaw, Authentication and quantitative analysis on the chemical profile of cassia bark (*Cortex cinnamomi*) by high-pressure liquid chromatography, J. Agr. Food Chem. 53 (2005) 2424–2428.
[6] Y.H. Kong, Y.O. Jo, C.W. Cho, D. Son, S. Park, J. Rho, S.Y. Choi, Inhibitory effects of cinnamic acid on melanin biosynthesis in skin, Biol. Pharm. Bull. 31 (2008) 946–954.
[7] Z. Sheng, S. Ge, X. Xu, Y. Zhang, P. Wu, K. Zhang, X. Xu, C. Li, D. Zhao, X. Tang, Design, synthesis and evaluation of cinnamic acid ester derivatives as mushroom tyrosinase inhibitors, Medchemcomm 9 (2018) 853–861.
[8] S. Ullah, D. Kang, S. Lee, M. Ikram, C. Park, Y. Park, S. Yoon, P. Chun, H.R. Moon, Synthesis of cinnamic amide derivatives and their anti-melanogenic effect in alpha-MSH-stimulated B16F10 melanoma cells, Eur. J. Med. Chem. 161 (2019) 78–92.
[9] S. Ullah, Y. Park, M. Ikram, S. Lee, C. Park, D. Kang, J. Yang, J. Akter, S. Yoon, P. Chun, H.R. Moon, Design, synthesis and anti-melanogenic effect of cinnamamide derivatives, Bioorg. Med. Chem. 26 (2018) 5672–5681.
[10] H.D. Zhan, H.Y. Zhou, Y.P. Sui, X.L. Du, W.H. Wang, L. Dai, F. Sui, H.R. Huo, T.L. Jiang, The rhizome of *Gastrodia elata* Blume – an ethnopharmacological review, J. Ethnopharmacol. 189 (2016) 361–385.
[11] W.C. Chen, T.S. Tseng, N.W. Hsiao, Y.L. Lin, Z.H. Wen, C.C. Tsai, Y.C. Lee, H.H. Lin, K.C. Tsai, Discovery of highly potent tyrosinase inhibitor, T1, with significant anti-melanogenesis ability by zebrafish *in vivo* assay and computational molecular modeling, Sci. Rep. 5 (2015) 7995–8002.
[12] E. Shim, E. Song, K.S. Choi, H.J. Choi, J. Hwang, Inhibitory effect of Gastrodia elata Blume extract on alpha-melanocyte stimulating hormone-induced melanogenesis in murine B16F10 melanoma, Nutr. Res. Pract. 11 (2017) 173–179.
[13] S. Wang, M. Bilal, H. Hu, W. Wang, X. Zhang, 4-Hydroxybenzoic acid-a versatile platform intermediate for value-added compounds, Appl. Microbiol. Biot. 102 (2018) 3561–3571.
[14] S.H. Liu, I.H. Pan, I.M. Chu, Inhibitory effect of p-hydroxybenzyl alcohol on tyrosinase activity and melanogenesis, Biol. Pharm. Bull. 30 (2007) 1135–1139.
[15] J.L. Gonzalez-Alfonso, P. Penalver, A.O. Ballesteros, J.C. Morales, F.J. Plou, Effect of alpha-glucosylation on the stability, antioxidant properties, toxicity, and neuroprotective activity of (-)-epigallocatechin gallate, Front. Nutr. 6 (2019) 30–38.
[16] T. Noor Mohammadi, A.T. Maung, J. Sato, T. Sonoda, Y. Masuda, K. Honjoh, T. Miyamoto, Mechanism for antibacterial action of epigallocatechin gallate and theaflavin-3,3'-digallate on *Clostridium perfringens*, J. Appl. Microbiol. 126 (2019) 633–640.
[17] D.S. Kim, S.H. Park, S.B. Kwon, K. Li, S.W. Youn, K.C. Park, (-)-Epigallocatechin-3-gallate and hinokitiol reduce melanin synthesis via decreased MITF production, Arch. Pharm. Res. 27 (2004) 334–339.

[18] B.N. Chen, R. Xing, F. Wang, A.P. Zheng, L. Wang, Inhibitory effects of α-Na 8 SiW 11 CoO 40 on tyrosinase and its application in controlling browning of fresh-cut apples, Food Chem. 188 (2015) 177–183.
[19] M.Z. Lin, W.M. Chai, O.Y. Chong, Q. Huang, X.H. Xu, Y.Y. Peng, Antityrosinase mechanism of omeprazole and its application on the preservation of fresh-cut Fuji apple, Int. J. Biol. Macromol. 117 (2018) 538–545.
[20] G.E. Ibrahim, I.M. Hassan, A.M. Abd-Elrashid, K.F. El-Massry, A.H. Eh-Ghorab, M.R. Manal, F. Osman, Effect of clouding agents on the quality of apple juice during storage, Food Hydrocolloid. 25 (2011) 91–97.
[21] M. Ruslan, A. Valente, S.A. Barringer, The effect of antibrowning agents on inhibition of potato browning, volatile organic compound profile, and microbial inhibition, J. Food Sci. 77 (2012) 1234–1240.
[22] C.Y. Chen, X.D. Wei, C.R. Chen, 3,4,5-Trimethoxycinnamic acid, one of the constituents of *Polygalae Radix* exerts anti-seizure effects by modulating GABAAergic systems in mice, J. Pharmacol. Sci. 131 (2016) 1–5.
[23] Z. Zhao, H. Song, J. Xie, T. Liu, X. Zhao, X. Chen, X. He, S. Wu, Y. Zhang, X. Zheng, Research progress in the biological activities of 3,4,5-trimethoxycinnamic acid (TMCA) derivatives, Eur. J. Med. Chem. 173 (2019) 213–227.
[24] Y. Cui, Y.H. Hu, F. Yu, J. Zheng, L.S. Chen, Q.X. Chen, Q. Wang, Inhibition kinetics and molecular simulation of p-substituted cinnamic acid derivatives on tyrosinase, Int. J. Biol. Macromol. 95 (2017) 1289–1297.
[25] H. Hridya, A. Amrita, M. Sankari, C. George Priya Doss, M. Gopalakrishnan, C. Gopalakrishnan, R. Siva, Inhibitory effect of brazilein on tyrosinase and melanin synthesis: kinetics and in silico approach, Int. J. Biol. Macromol. 81 (2015) 228–234.
[26] L.L. Shao, X.L. Wang, K. Chen, X.W. Dong, L.M. Kong, D.Y. Zhao, R.C. Hider, T. Zhou, Novel hydroxypyridinone derivatives containing an oxime ether moiety: synthesis, inhibition on mushroom tyrosinase and application in anti-browning of fresh-cut apples, Food Chem. 242 (2018) 174–181.
[27] B.N. Chen, R. Xing, F. Wang, A.P. Zheng, L. Wang, Inhibitory effects of alpha-Na8SiW11CoO40 on tyrosinase and its application in controlling browning of fresh-cut apples, Food Chem. 188 (2015) 177–183.
[28] M.A. Rojas-Grau, R. Soliva-Fortuny, O. Niartin-Belloso, Effect of natural anti-browning agents on color and related enzymes in fresh-cut Fuji apples as an alternative to the use of ascorbic acid, J. Food Sci. 73 (2008) S267–S272.
[29] M. Chiumarelli, M.D. Hubinger, Stability, solubility, mechanical and barrier properties of cassava starch – Carnauba wax edible coatings to preserve fresh-cut apples, Food Hydrocolloid. 28 (2012) 59–67.
[30] M.F. Mahomoodally, G. Zengin, D. Zheleva-Dimitrova, A. Mollica, A. Stefanucci, K.I. Sinan, M.Z. Aumeeruddy, Metabolomics profiling, bio-pharmaceutical properties of *Hypericum lanuginosum* extracts by in vitro and in silico approaches, Ind. Crop. Prod. 133 (2019) 373–382.
[31] G. Karakaya, A. Ture, A. Ercan, S. Oncul, M.D. Aytemir, Synthesis, computational molecular docking analysis and effectiveness on tyrosinase inhibition of kojic acid derivatives, Bioorg. Chem. 88 (2019) 102950–102960.
[32] M.N. Mustafa, A. Saeed, P.A. Channar, F.A. Larik, M. Zain-Ul Abideen, G. Shabir, Q. Abbas, M. Hassan, H. Raza, S.Y. Seo, Synthesis, molecular docking and kinetic studies of novel quinolinyl based acyl thioureas as mushroom tyrosinase inhibitors and free radical scavengers, Bioorg. Chem. 90 (2019) 103063–103071.
[33] Z. Zhao, Y. Bai, J. Xie, X. Chen, X. He, Y. Sun, Y. Bai, Y. Zhang, S. Wu, X. Zheng, Excavating precursors from the traditional Chinese herb *Polygala tenuifolia* and *Gastrodia elata*: synthesis, anticonvulsant activity evaluation of 3,4,5-trimethoxycinnamic acid (TMCA) ester derivatives, Bioorg. Chem. 88 (2019) 102832–102840.
[34] T. Mosmann, Rapid colorimetric assay for cellular growth and survival: application to proliferation and cytotoxicity assays, J. Immunol. Methods 65 (1983) 55–63.
[35] M. Mohammadi-Khanaposhtani, M. Shabani, M. Faizi, I. Aghaei, R. Jahani, Z. Sharafi, N. Shamsaei Zafarghandi, M. Mahdavi, T. Akbarzadeh, S. Emami, A. Shafiee, A. Foroumadi, Design, synthesis, pharmacological evaluation, and docking study of new acridone-based 1,2,4-oxadiazoles as potential anticonvulsant agents, Eur. J. Med. Chem. 112 (2016) 91–98.
[36] P. Wu, Y. You, Y. Liu, C. Hou, C. Wu, K. Wen, C. Lin, H. Chiang, Sesamol inhibited melanogenesis by regulating melanin-related signal transduction in B16F10 Cells, Int. J. Mol. Sci. 19 (2018) 1908–11121.
[37] S.M. Son, K.D. Moon, C.Y. Lee, Kinetic study of oxalic acid inhibition on enzymatic browning, J. Agric. Food Chem. 48 (2000) 2071–2074.
[38] D. Sousa-Pereira, O.A. Chaves, C.M. Dos Reis, M.C.C. de Oliveira, C.M.R. Sant'Anna, J.C. Netto-Ferreira, A. Echevarria, Synthesis and biological evaluation of N-aryl-2-phenyl-hydrazinecarbothioamides: experimental and theoretical analysis on tyrosinase inhibition and interaction with HSA, Bioorg. Chem. 81 (2018) 79–87.
[39] W.T. Ismaya, H.J. Rozeboom, A. Weijn, J.J. Mes, F. Fusetti, H.J. Wichers, B.W. Dijkstra, Crystal structure of *Agaricus bisporus* mushroom tyrosinase: identity of the tetramer subunits and interaction with tropolone, Biochemistry 50 (2011) 5477–5486.
[40] T. Pillaiyar, V. Namasivayam, M. Manickam, S.H. Jung, Inhibitors of melanogenesis: an updated review, J. Med. Chem. 61 (2018) 7395–7418.